

Extrusion-Based Differences in Two Types of Nylon 6 Capillary-Channeled Polymer (C-CP) Fiber Stationary Phases as Applied to the Separation of Proteins via Ion Exchange Chromatography

Abby J. Schadock-Hewitt,¹ Jennifer J. Pittman,¹ Kathryn A. Stevens,² R. Kenneth Marcus¹

¹Department of Chemistry, Biosystems Research Complex, Clemson University, Clemson, South Carolina 29633

²School of Materials Science and Engineering, Clemson University, Clemson, South Carolina 29634

Correspondence to: R. K. Marcus (E-mail: marcusr@clemson.edu)

ABSTRACT: Nylon 6 capillary-channeled polymer (C-CP) fibers used as the stationary phase in high-performance liquid chromatography protein separations have been investigated. A difference in chromatographic behavior between two (presumably identical) nylon 6 C-CP fibers, designated simply as nylon 6A and nylon 6B, reveals unknown differences in their chemical and physical nature as proteins are less retained on the latter. The possible differences are evaluated through several test methods, including Fourier transform infrared spectroscopy (FTIR), differential scanning calorimetry (DSC), mechanical testing, MALDI-TOF mass spectrometry, an organic reaction with ninhydrin, and dilute solution viscometry. Nylon 6B is shown to be a larger perimeter, stronger fiber, yet in a 200 mm, 0.8 mm i.d. column having an interstitial fraction of ~ 0.6 , it has an available surface area of ~ 189 cm², while nylon 6A is almost double that at ~ 374 cm². It is revealed that when in amorphous form, the base polymers have very comparable FTIR and DSC characteristics. When in their solid, extruded fiber form there are significant differences found in crystallinity, tensile strength, molecular weight distribution, and end group density. Nylon 6A is a lower molecular weight fiber, which results in $\sim 1.3\times$ more amine end groups than nylon 6B. It is the end group density that ultimately determines the separation qualities. These results imply that both a difference in base nylon 6 molecular weight and also the fiber extrusion process have a significant influence on the performance of nylon 6 C-CP fiber separation of proteins via ion exchange chromatography. © 2012 Wiley Periodicals, Inc. *J. Appl. Polym. Sci.* 000: 000–000, 2012

KEYWORDS: fibers; extrusion; proteins; separation techniques; properties; characterization

Received 26 March 2012; accepted 23 August 2012; published online

DOI: 10.1002/app.38509

INTRODUCTION

Nylon is among the most common commercially used synthetic fibers, having a wide range of textile and industrial applications.^{1–4} Nylon is advantageous over other textile polymers due to its robustness, chemical versatility, dyeability, unique wettability (high hydrophilicity), as well as overall chemical and thermal stability. These features lead to the use of nylon in a variety of chemical manipulations such as a protein immobilization support in the form of membranes,^{5,6} and particles^{7,8} for chemical separations and fluorescence measurements. Nylon-based materials have also been used in the form of nanofibrous membranes for water filtration, effectively isolating 90% of 0.5 μm particles from flowing streams.⁹ While there are several chemical forms of nylon, nylon 6, named for the 6 carbons between each amide in the polymer backbone, is used most often as a chemical support because of its more open and random

structure, allowing for more rapid and uniform functionalization. Nylon 6 (poly(Σ -caprolactam)) is an AB type linear polyamide, formed through the aqueous polymerization of the cyclic amide caprolactam. For the above applications, nylon 6 is relatively cheap when compared to similar supports, is readily available, has an active surface for interactions with analytes of interest, and provides for ready surface chemical modification for attachment of species-specific ligands. As a drawback, nylon 6 precipitated to form bead supports must be activated to generate the desired amine and carboxyl groups on its surface; however, most membranes and fibers require no such pretreatments prior to use.

It seems advantageous to develop a nylon fiber support that can also be used as a stationary phase for high performance liquid chromatography (HPLC) separations, requiring no pretreatment, with the ability to effectively separate several proteins in

Additional Supporting Information may be found in the online version of this article.

© 2012 Wiley Periodicals, Inc.

a mixture. Marcus has reviewed the application of fibrous stationary phases in liquid chromatography, where common traits include low materials costs, ease of column fabrication, presentation of diverse surface chemistries, efficient fluid mass transit through columns, and effective solute mass transfer to and from the stationary phase surface through convective diffusion processes.^{10,11} In this laboratory, we are currently focused on the characterization of capillary-channeled polymer (C-CP) fibers utilized as a combined support/stationary phase for protein separations by HPLC. These fibers exhibit a higher surface area versus circular cross-section fibers due to their unique shape, consisting of eight capillary channels that run axially down the length of the fiber. In terms of biomolecule separations, the fibers are essentially nonporous and exhibit very efficient mass transfer properties; as such, effective separations can be performed at high linear velocities ($>25 \text{ mm s}^{-1}$) with low backpressures ($<1500 \text{ psi}$).

C-CP fibers have been studied extensively and have been applied in many different chromatographic modes including reversed-phased (RP), ion exchange (IEX), hydrophobic interaction (HIC), and mixed-mode chromatographies.^{10–18} These different modes are readily affected by the choice of base polymer identity among polypropylene (PP), poly(ethylene terephthalate) (polyester, PET), and nylon 6. In 2003, Marcus et al. first demonstrated the combined support/stationary phase ability of PP and PET C-CP fibers in RP separations of polyaromatic hydrocarbons (PAHs), organic and inorganic lead, amino acids, and lipids.¹² PP and PET C-CP columns, when compared with a commercially available C_4 -derivatized silica column for the separation of proteins, showed increased repeatability of peak width and retention time, greater recoveries, and the potential for ultrafast separations.^{13,14} Rapid protein separations were further studied with optimal peak resolution achieved with a 2.1 mm i.d. PET column at a flow rate of 7 mL/min.¹⁵ Smaller i.d. PP microbore columns (1000 mm in length) were shown to achieve high column efficiency while maintaining relatively low backpressures.¹⁶ Most recently, nylon 6 C-CP columns were shown to effectively separate proteins at comparatively high linear velocities ($\sim 21 \text{ mm/s}$) by a mixed-mode IEX/RP chromatography¹⁷ and excellent resolution with fast analysis times achieved by HIC.¹⁸ Overall, C-CP fiber columns have continuously been shown to provide high efficiency separations at high linear velocities and high recoveries in comparison to derivatized silica phases, which are the industry standards.¹⁵

The nylon 6 C-CP fibers are similar to commonly used membrane and bead-form supports because they are cheap, easily made, and readily available.^{2–4} Unlike analogs polyamide particles, nylon 6 fibers do not require activation to generate surface functional groups. When nylon 6 bulk polymers are extruded into fibers various degradation processes lead to a discontinuity of the polymer chains, exposing the amine and carboxyl surface functional groups. It is these end groups that contribute to the hydrophilicity of the surfaces (allowing for effective HIC separations) and provide cationic and anionic sites to affect IEX separations as described here.¹⁸ The nylon 6 C-CP fibers enable electrostatic interactions between the charged amino acids making up the outer portions of a protein

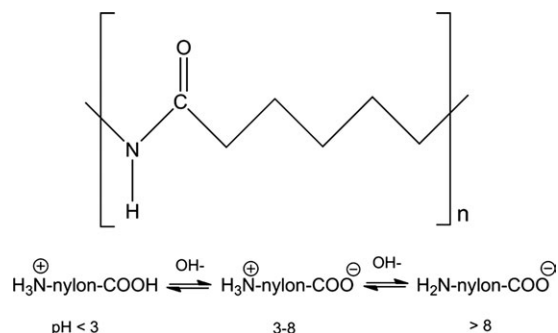


Figure 1. Nylon 6 monomer structure and the effects of pH on the end group functionality.

molecule and the charged end groups ($-\text{NH}_3^+$ and $-\text{COO}^-$) of the amide polymer. The mixed-mode nature of separation involves additional interactions between hydrophobic portions of proteins with the alkyl chains making up the polymer backbone. An underappreciated aspect of the use of nylon 6 as an extraction/chromatographic support is the level of “surface tunability” that can be affected due to the zwitterionic nature of the end groups. As such, nylon 6 C-CP fibers can be used for both anion- and cation-exchange separations based on the solvent pH, as illustrated in Figure 1. As indicated, the nylon 6 surface is cationic in nature at low pH (making it useful for anionic exchange), with the surface charge being a net negative at $\text{pH} > 8$ (allowing for separations based on cation exchange).

Not unlike other types of chromatographic stationary phases, HPLC separations on C-CP fiber columns are first dictated by the chemical nature of the fiber surfaces as this determines the types and strengths of the protein-surface interactions. The specific fiber shape, perimeter, denier, and column packing density in turn affect the column hydrodynamics and the available surface area for interaction. Even in the case of identical monomers, subtle differences may be manifest due to inconsistencies in the base nylon 6 polymers used for fiber extrusion. It is known that nylon performance (in general) is based on a variety of properties, including amide content (molecular weight), crystallinity, and melting point. Because of their linear discerned symmetry, nylon 6 fibers show high crystallinity that varies based on extrusion processes.¹⁹ We describe here a comprehensive evaluation of the chemical and physical attributes of two nylon 6 C-CP fiber stocks (referred to as nylon 6A and nylon 6B), which affect their performance in the IEX chromatography separation of a simple three-protein suite of ribonuclease A, cytochrome c, and lysozyme. Attenuated total reflectance Fourier transform infrared spectroscopy (ATR-FTIR) and differential scanning calorimetry (DSC) provide insight into the base polymer and amorphous/crystalline structure of the nylon 6. MALDI-TOF mass spectra of the surface of fibers dissolved in trifluoroethanol (TFE) also provide confirmation of the identities of the base monomers. Mechanical properties discerned from tensile testing allow for information regarding the fiber extrusion process. Relative viscometry of the fibers was measured and used to calculate a number average molecular weight. As a final test, end group densities were quantitatively determined by a reaction with ninhydrin, which causes a

Table I. Physical Property Differences Between Nylon 6 C-CP Fibers

Sample	Filaments/yarn	DPF	Perimeter (μm)	Surface Area/ Column (cm^2)	Average mass/ column (mg)
Nylon 6A	30	2.67	207.5	373.5	7.76 ± 0.02
Nylon 6B	25	7.74	270.7	189.5	8.25 ± 0.02

photometrically measurable color change in the presence of amide groups, and serves to complement MALDI data, relating molecular weight and end group density. As a whole, this insight into the physical and chemical characteristics of C-CP fibers alludes to a greater understanding of their properties and future performance optimization. Regardless of the actual identity of the materials evaluated here, the results point to the need to critically evaluate the roll of differing base polymers and fiber extrusion conditions in the ultimate chemical character of the fiber surfaces, and thus their separation qualities.

EXPERIMENTAL

Chemicals, Reagents, and Standards

HPLC-grade acetonitrile (ACN) and HPLC-grade methanol, used to clean the fibers, and 2-propanol (isopropanol) and ethanol, used in the ninhydrin reaction, were obtained from Fisher Scientific, (Pittsburgh, PA). Milli-Q water ($18.2 \text{ M}\Omega \text{ cm}^{-1}$) derived from a Millipore water system (Billerica, MA) was used for fiber rinsing and preparation of TRIS-HCl buffer, ammonium chloride (NH_4Cl) salt solutions, and all other aqueous-based solutions. One molar Tris-HCl, pH 8.0, was purchased from Teknova (Hollister, CA) and diluted appropriately into 20 mM Tris-HCl, pH 8, employed as mobile phase, buffer A. One molar NH_4Cl in 20 mM Tris-HCl was used as the elution buffer, buffer B. A standard three-protein stock solution was prepared in 20 mM Tris-HCl buffer at pH 8.0, at a concentration of 0.25 mg mL^{-1} for each protein. The suite included ribonuclease A (RNase A) ($M_W = 13.7 \text{ kDa}$), cytochrome c (cyto c) ($M_W = 12.4 \text{ kDa}$), and lysozyme ($M_W = 14.3 \text{ kDa}$), all having isoelectric points (pI) above the physiological pH = 7.4, and so referred to as basic. The protein solutions were stored at

6°C . Pyridine, propionic acid, sodium propionate, 2-methoxyethanol, ϵ -aminocaproic acid, and ninhydrin, all used in the ninhydrin reaction, and the 2-(4-Hydroxyphenylazo)benzoic acid (HABA) matrix species for MALDI-MS, and the TFE used to dissolve fibers prior to MALDI-MS analysis, were purchased from Sigma Aldrich (Milwaukee, WI).

Physical Property Considerations and Column Preparation

Nylon 6 C-CP fibers were obtained from the Clemson University School of Materials Science and Engineering (Clemson, SC) (nylon 6A) and Fiber Innovations Technology (FIT, Johnson City, TN) (nylon 6B). Bundles of fibers were prepared and pulled through 0.8 mm i.d., 200 mm long fluorinated ethylene propylene (FEP) tubing (Cole-Parmer, Vernon Hills, IL) as previously described to form microbore format C-CP fiber columns.^{12,13} The perimeter, weight, denier, and total surface area are provided in Table I. The fiber perimeter was determined through a mathematical program using the SEM cross-section images of the fibers (Figure 2). The denier per filament (dpf) was determined by calculating fiber weight in grams per 9000 m. Bobbins of nylon 6A were wound as 30 filaments per fiber bundle, while nylon 6B has 25 filaments per fiber. On the basis of previous results,¹³ the nylon 6 C-CP fiber columns were packed to yield interstitial fractions of $\epsilon_i \cong 0.6$ (i.e., ~60% void volume). In this case, 900 nylon 6A fibers and 350 nylon 6B fibers were pulled through the FEP tubing, respectively. The actual column void volumes were determined by injection of an unretained compound, uracil (0.1 mg mL^{-1}).²⁰ The total surface area of fibers, reported in Table I, was calculated by multiplying column length, fiber perimeter, and the number of individual filaments in the column. Once pulled through the column, the fibers were trimmed with a surgical scalpel to be

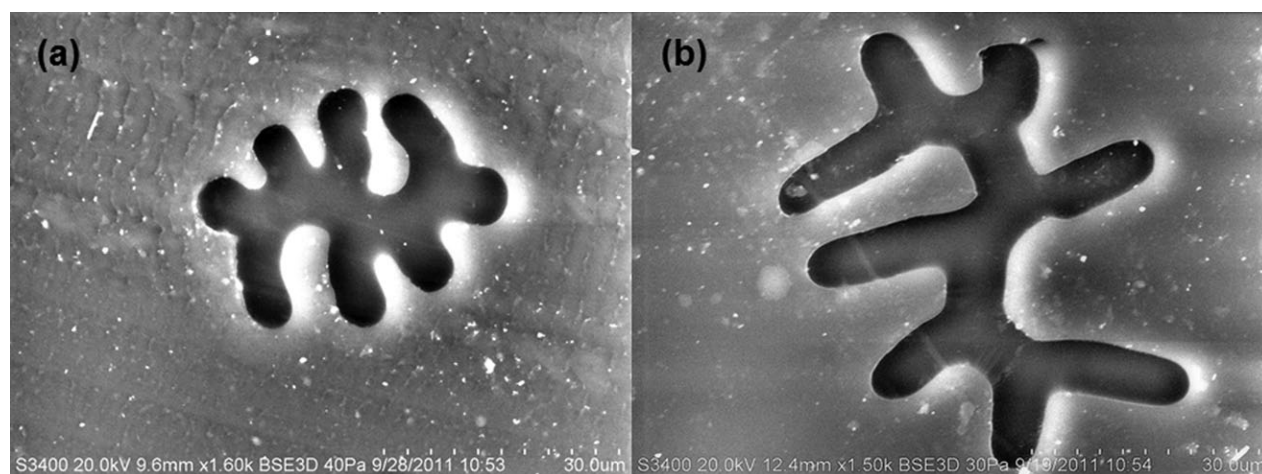


Figure 2. SEM cross-sectional images of nylon 6 C-CP fibers (a) nylon 6A and (b) nylon 6B.

flush with the tubing ends. Before performing separations, columns were completed with end fittings (Valco Instruments, Houston, TX) and PEEK unions (VWR International, West Chester, PA), allowing for connection to the HPLC system for fiber/column washing. Successive wash solutions beginning with 100% ACN, followed by 100% hexane, 100% methanol, and finally 100% DI-H₂O, were pumped through the capillary column (1 mL min⁻¹). Each solvent was flushed until a stable baseline absorbance signal was achieved for at least 10 min.

Chromatographic System and Operations

The chromatographic system consisted of a Dionex (Sunnyvale, CA) Ultimate 3000 with a model LPG-3400SD pump, a WPS-3000TSL autosampler, and a VWD-3400 RS variable wavelength UV-VIS absorbance detector, operated at 216 nm. The Dionex Chromeleon software was used to generate data for the chromatograms, and further analysis was done through Microsoft (Seattle, WA) Excel. C-CP fiber columns were washed, prior to experimental runs, with 100% acetonitrile until a stable baseline absorbance is reached, then 100% milli-Q water until a stable baseline value was achieved, and finally equilibrated with 100% 20 mM Tris-HCl (buffer A) while the baseline remained stable. Each protein mixture injection was performed at 2 mL min⁻¹ 100% buffer A with a 2 min equilibration between injections. No difference was seen in chromatograms when a hold time of 1 min was added before gradient initiation and when it was not. Optimal protein elution was found at a gradient of 0–50% 1M NH₄Cl in 20 mM Tris-HCl in 2 min. In doing so, the proteins are sequentially eluted through a displacement mechanism wherein the cationic groups of the proteins are substituted by the increasing ammonium ion (NH₄⁺) content in the mobile phase. While single chromatograms are presented to illustrate the separation characteristics of the respective fibers, triplicate repetitions do indeed yield agreements in retention times of better than 5%, relative.

Scanning Electron Micrographs

Micrograph cross-sectional images of nylon 6A and nylon 6B were taken on a Hitachi S-3400-N (Hitachi Scientific Instruments, Pleasanton, CA) scanning electron microscope (SEM) system. Single fibers were mounted vertically, suspended in a resin, and one end cut smooth with a RMC Powertome X (Boeckler Instruments, RMC Products, Tucson, AZ) microtome before being mounted on a standard stainless steel SEM platform using double-sided graphite tape in a near-vertical position. Images were taken at an accelerating voltage of 20 kV with image magnifications of 1500–1600 \times .

Attenuated Total Reflection FTIR (ATR-FTIR) Spectroscopy

ATR-FTIR measurements were performed on washed and air-dried nylon 6 C-CP fibers using a Thermo-Nicolet Magna 550 FTIR spectrometer equipped with a single bounce Thermo-Spectra-Tech Foundation Series Diamond ATR with a 50° angle of incidence. The fibers were force-pressed onto the diamond crystal to ensure maximum contact. Generated spectra were an accumulation of 16 scans with a resolution of 4 cm⁻¹. Data analysis and processing was performed using OMNIC ESP software, Version 6.1a.

Differential Scanning Calorimetry

A TA Instruments (New Castle, DE) MDSC 2920, equipped with a nitrogen cooling system was used to test the thermal properties of the fibers. Approximately 2 mg of the respective C-CP fibers were washed in the solvents as described above (ACN, hexane, methanol, and DI-H₂O) and air-dried prior to sealing in an aluminum pan. In quenching experiments, samples were initially heated from 0 to 300°C at a rate of 20°C min⁻¹. At 300°C the cell temperature was held constant while the sample was removed and quench-cooled on a stainless steel bar cooled with liquid nitrogen. After the cell was re-equilibrated to room temperature, the quenched sample was reintroduced. The second DSC analysis was performed identically to the first, with heating from ~25 to 300°C at 20°C min⁻¹. DSC was also performed without quench cooling to confirm melting temperature and heat capacity. The acquisition software used was TA Instruments Thermal Advantage, Version 1.1A. Data were analyzed using TA Instruments Universal Analysis 2000, Version 3.9A. Samples of each fiber type were run in triplicate for each DSC process.

Matrix Assisted Laser Desorption Ionization Time-of-Flight Mass Spectrometry (MALDI-TOF-MS)

MALDI analysis was performed on a Bruker Daltonics (Billerica, MA) microflex LRF, MALDI-TOF mass spectrometer in the positive ion (160 ns delay), reflectron mode. The system is equipped with a nitrogen laser (337 nm) operating at a pulse rate of 60 Hz. A 72% laser power was used throughout the studies, with the spectra presented being a summation of 300 laser shots per position. A mass range of 260–3000 *m/z* was suitable. Fibers were tested in triplicate as TFE-dissolved samples as a means to assess the “original” polymer/monomer identities. In this case, 1 μ L of the sample was sandwiched between two 1 μ L drops of HABA as the matrix; each drop was pipetted onto the target and left to dry before addition of the subsequent layer.

Mechanical Properties

The mechanical properties, such as the modulus, tenacity, and extension at break of the washed and air-dried fibers were determined from their load elongation curves. Tensile testing was performed using an Instron 5582 (Canton, MA). ASTM2256 was utilized to obtain the elongation, modulus, and tenacity of the yarn samples. A gauge length of 25 mm was employed for yarn testing and the cross head speed set such that fiber breakage occurred in 20 \pm 2 s. Ten samples of each yarn were analyzed and the average and standard deviation was calculated for elongation, modulus, and tenacity in each case.

Dilute Solution Viscometry

The molecular weights (\bar{M})_n of the respective polymers were assessed through the relative viscosity (RV) of each fiber type, determined in 90% formic acid at 25°C using an Ostwald viscometer size B. A 1% solution (wt/wt) was prepared for both nylon samples and the flow time compared to that of pure solvent. The flow times were recorded until the measurements were reproducible to \pm 0.2 s. The RV was calculated using the following equation:

$$RV = t/t_0 \quad (1)$$

where *t* is the average flow time of the test solution and *t*₀ is the average flow time of the neat solvent.

Ninhydrin Analysis Technique

The amine end group content was determined through the ninhydrin technique, as described by Knott and Rossbach.²¹ Fiber samples were prepared in the same manner as for column preparation, using 20 mg of each fiber type and the same series of solvents (ACN, hexane, methanol, and DI-H₂O), followed by air drying prior to analysis. Each sample was placed in a 50-mL round-bottom flask with 1 mL of 10% isopropanol, 1 mL of 10% pyridine, and 2 mL of a reagent solution of 9.3 mL propionic acid, 20.18 g sodium propionate, 50 mL methylcellosolve, and 2 g of ninhydrin filled to 100 mL with water. The flask was stoppered and the mixture heated for 30 min in a boiling water bath. Twenty milliliters of 50% ethanol was added to the mixture and the flask was shaken then left to sit for 15 min. The fibers were removed from the mixture and pressed at the end of a syringe to ensure that the vast majority of liquid was removed. The liquid remaining in the flask was quantitatively transferred into a 100-mL volumetric flask and filled to the mark with water. Each fiber type was analyzed in triplicate with a $2 \times 10^{-6}M$ solution of ϵ -aminocaproic acid analyzed in parallel to the fibers as a calibrant. A reaction containing no fibers or ϵ -aminocaproic acid was used as a blank with the quantitative absorbance measurements performed at the $\lambda_{\max} = 570$ nm.

RESULTS AND DISCUSSION

Physical Characteristics of Fibers/Columns

As described previously, the respective fiber columns were composed to yield interstitial fractions of $\epsilon_i \cong 0.6$. In considering the capillary tubing (200×0.8 mm i.d.), creating this interstitial fraction required 30 column lengths of nylon 6A fiber, with 30 filaments per fiber bundle giving a total of 900 fibers running lengthwise down the column. For the larger nylon 6B, which has 25 fibers per bundle, only 14 column lengths or 350 total filaments were required to yield very similar void volumes. In terms of total fiber mass, the 900 nylon 6A fibers weighed 7.76 mg, and the 350 fibers of nylon 6B weighed 8.25 mg. However, while there is more total polymer fiber in the latter column, a more important figure of merit in terms of chemical separations is the accessible surface area, at which chemical interactions can occur. To be clear, on the size scale of proteins, the pore sizes in these extruded fibers are such that only “surface” interactions are occurring. SEM imaging, shown in Figure 2, reveals the relative size and perimeter differences of the fibers. Shown on the same 30- μ m scale, nylon 6B [Figure 2(b)] takes up almost $2\times$ the area of nylon 6A [Figure 2(a)], also having deeper, wider channels. In support of the obvious visual difference, nylon 6B is $\sim 25\%$ larger in perimeter than nylon 6A, as noted in Table I. Although nylon 6B has a larger perimeter than nylon 6A, the total surface area in the column based on the number of fibers needed for efficient column packing tells the opposite story, as the total available fiber surface area for the nylon 6A column is nearly twice that of the higher dpf fiber column. In dealing with interactions that occur primarily on the fiber surface, this insight is significant when considering chromatographic separation qualities. On a first-principles basis, a column with $2\times$ greater surface area suggests a higher propensity for solute-surface interactions affecting high separation efficiencies.

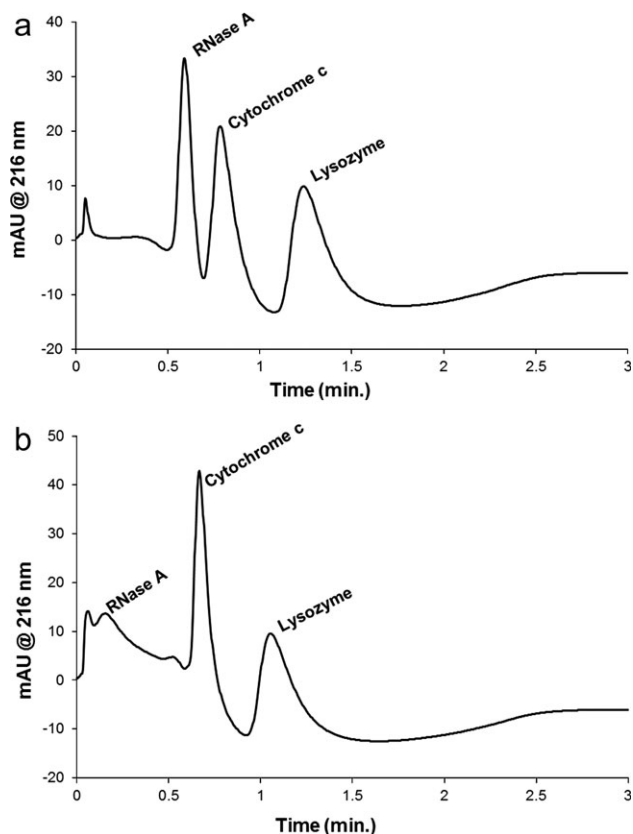


Figure 3. Separation of ribonuclease A, cytochrome c, and lysozyme on (a) nylon 6A C-CP and (b) nylon 6B C-CP fiber columns (gradient conditions in text).

Protein Separation

The protein mixture of ribonuclease A, cytochrome c, and lysozyme was first separated on the nylon 6A C-CP fiber packed column using a mobile phase of 20 mM Tris-HCl buffer at pH 8, with an optimized gradient program of 0–50% 1M ammonium chloride in 20 mM Tris-HCl over 2 min at a flow rate of 2 mL min^{-1} . The chromatogram in Figure 3(a) displays an efficient separation with fully resolved peaks in elution order of RNase A at 0.58 min, cyto c at 0.78 min, and lyso at 1.21 min. Protein identity was confirmed by single-solute injections. This order is reflective of each protein’s isoelectric point (pI) (RNase A pI = 8.7, cyto c pI = 10.0, lysozyme pI = 11.0), which hints at the density of the charged groups available on the protein as a function of the mobile phase pH. At pH 8, all three proteins have a net positive charge, and are thus displaced by the increasing ammonium ion concentration. While the net charge of the protein is not fully descriptive of the retention characteristics of the proteins, it does suggest that RNase A is the least retained due to the small ratio between its pI and the solvent pH, being the least cationic (i.e., having the smallest number of protonated surface amine groups) of the three proteins. The elution order thus (loosely) follows the number of cationic/acid groups at pH = 8.

Figure 3(b) shows the separation of the same three-protein suite on a nylon 6B C-CP fiber packed column under the same gradient conditions as for nylon 6A. Resolved peaks from cyto c and

lyso are seen at shorter retention times of 0.66 and 1.03 min, respectively, while RNase A is mostly unretained, and is seen as a continuation of the solvent/injection peak at $t_0 \sim 0.05$ min. The broad band from $t \sim 0.13$ – 0.50 min suggests that any RNase A retention was due to HICs and very little electrostatic interaction occurred with the nylon 6B surface. In practice, even if the protein has a net charge of 0 (i.e., pH = PI), this only implies that there are an equal number of positive and negative charges, with the equilibrium value determined by the precise pH. Also important here, is the fact that even in the absence of any protein or surface charge, there are HICs, which may affect some level of retention, if only slightly. The combination of loss of RNaseA retention and the shorter retention times for cyto c and lyso points to an overall loss of surface activity; i.e., access to a lower surface charge density.

In comparing Figure 3(a, b), it is curious that two forms of nylon 6 fibers produce such different chromatograms. It is understood that physical differences manifest in the column hydrodynamics might affect the quality of the protein elution profiles (principally peak widths and shapes), but such differences would not affect the chemical nature of the separations in terms of degree of column retention. As much of the chemical/physical information about the fibers was unknown, it was important to delve deeper into the cause of these chromatographic differences on seemingly chemically equivalent materials. The studies described here are directed at gaining greater levels of understanding as to how extrusion and molecular weight based differences may affect the chemical nature of what *should be* an identical separation.

Chemical and Physical Structural Characterization

FTIR. As a first step, it was necessary to confirm the basic chemical identity of the two fibers under study. More specifically, characteristic amide, amine, and carboxyl groups present in the nylon 6 fibers are easily identified through FTIR spectroscopy. FTIR is an essential method for polymer characterization, and the availability of reference nylon FTIR spectra makes comparisons easy. Fourier transform infrared spectra were taken for nylon 6A and 6B; included in Supporting Information, Figure S1. Characteristic nylon 6 bands are seen for both. An N–H stretch band is seen from 3356 to 3180 cm^{-1} and the C=O (amide I) stretch band is seen from 1682 to 1579 cm^{-1} . A C–N stretch, N–H bend (amide II) band is seen from 1579 to 1483 cm^{-1} . An amide II overtone is seen at 3105 to 2989 cm^{-1} . C–H stretches are seen from 2976 to 2771 cm^{-1} . The amide III band is seen from 1272 to 1191 cm^{-1} . The C–C skeletal stretches are seen from 1192 to 1000 cm^{-1} . Comparison of these spectra with known nylon 6 absorbance bands served only to confirm that each fiber was made from a nylon 6 base polymer.^{22,23} Accordingly, as nylon 6A was extruded on-site we are absolutely confident that its source was nylon 6. Likewise, we are able to confirm that the nylon 6B C-CP fiber was *not* made from a nylon 6,6 base polymer (as one obvious alternative) due to the similarity between the two FTIR spectra; further testing described here supports this fact as well.

Thermal Analysis. The thermal characterization of the fibers was carried out via two modes of DSC to determine if crystal-

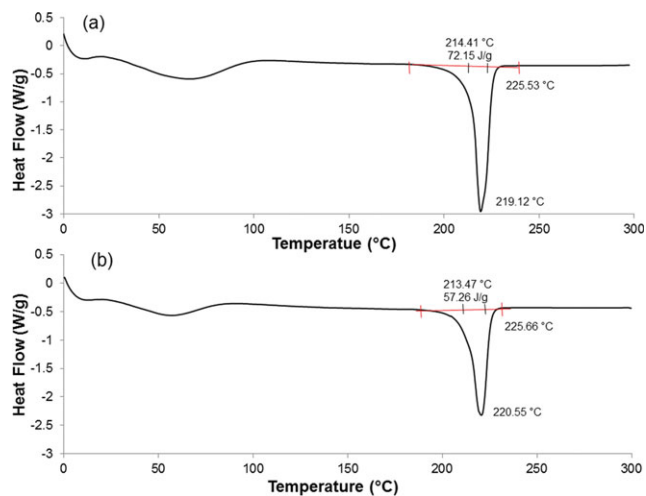


Figure 4. Direct DSC curves of (a) nylon 6A and (b) nylon 6B C-CP fibers. [Color figure can be viewed in the online issue, which is available at wileyonlinelibrary.com.]

linity differences existed between the samples. Crystallinity might be expected to impact separations in terms of access to the subsurface regions of the fibers. As seen in Figure 4, a broad endothermic peak observed between 5 and 60°C , which may be attributed to water loss, and unfortunately masked any information regarding the existence of a glass transition temperature (T_g). At T_g , the amorphous regions of a semicrystalline polymer change from a glassy state to a rubbery one. In other words, the polymer reaches a point where there is enough energy for the chain to begin to rotate around its bonds. To obtain an amorphous glassy material prior to DSC analysis, solid fibers are first melted and then quench-cooled. In this case, the transition from glassy to rubbery can be seen as both materials display very similar thermal characteristics as seen in Figure S2 of the Supporting Information. A step change in heat capacity occurs as the temperature rises. In S2a, T_g is seen from 6.5 to 42.1°C and likewise in S2b from 9.1 to 44.7°C for the two nylon fiber types. On the basis of this data, the T_g peaks should have occurred in the region of 40°C in Figure 4. No significant difference was observed in the initial DSC thermograms regarding the onset, offset, and midpoint temperatures of the melting exotherms with all three values lying in the expected range for nylon 6. The heat of melting (ΔH_m) was calculated by integrating the area under the melting peaks (Figure 4), which were found to be 72.15 and 57.26 J/g for nylon 6A and 6B, respectively. The percent crystallinity of each sample was then calculated using the following equation using theoretical heat of fusion for 100% crystalline nylon 6 of 230 J/g ,²⁴

$$\% \text{ crystallinity} = (\Delta H_m / \Delta H_c) \times 100 \quad (2)$$

where ΔH_m = heat of melting and ΔH_c = cold crystallization energy.

In this case, the DSC of neither sample reflected a cold crystallization peak, and so the values obtained from the integration of the melting endotherms were the sole input values. The degrees of crystallinity obtained were, 31.4% for nylon 6A and 24.9%

for nylon 6B. This was anticipated, as the denier per filament of the two samples were 2.64 and 7.74 for nylon 6A and nylon 6B, respectively. Lower denier fibers typically undergo more severe wind up conditions (i.e., higher wind up speed and tension), and so more crystallinity would be imparted to the smaller fibers. The 20% higher crystallinity in nylon 6A in comparison to nylon 6B gives insight into a potential to tailor fiber properties based on the extrusion process. In agreement with the IR data, when in their amorphous form after rapid quenching from the melt and subjected to the same DSC heating regime, nylon 6A and 6B both indicated thermal transitions characteristic of nylon 6, having T_g at $\sim 40^\circ\text{C}$, a crystallization temperature (T_c) at 68°C , and a melting temperature (T_m) at 220°C (Figure 4). This similarity in the thermal behavior via DSC did not highlight significant potential differences between the samples other than the crystallinity.

MALDI-TOF-MS. MALDI-MS was performed to provide insight into possible molecular weight differences between the two nylon 6 samples. In principle, the polymer molecular weight should be some reflection of the number of end groups available per unit area. While solid fiber analysis is uncommon, there is also little literature addressing MALDI-MS of nylon 6 fibers due to its insolubility in most common solvents such as tetrahydrofuran. To get around this, in some cases, a finely ground powder of sample and matrix is pressed into a pellet and analyzed in that form.²⁵ However, it is noted that this method was not accurate for end group determination, as disruption of end groups can occur during sample preparation. The groups of Montaudo et al.^{26,27} and Park and coworkers²⁸ report fully dissolving nylon 6 samples in TFE prior to MALDI analysis. They were able to obtain accurate mass values and end group distributions for several nylon 6 samples. MALDI mass spectra were obtained on the dissolved nylon 6A and 6B samples in an effort to ascertain the likelihood of them being extruded from the same molecular weight polymers. Figure S3 of the Supporting Information displays the MALDI-TOF mass spectra of samples that were fully dissolved in TFE prior to application to the MALDI target. While nylon 6B yielded a somewhat higher overall intensity, the m/z values for both spectra show nearly identical structure. Seen is a uniform oligomeric distribution having mass differences of ~ 113.1 Da between the respective families of peaks. This value is expected, as it is the molecular weight of the nylon 6 monomer (Figure 1), with the multiplets of peaks corresponding to oligomers having different numbers of monomer units. More specifically, the major peak in each multiplet represents ions of the form $[-\text{NH}-(\text{CH}_2)_5-\text{CO}]_n\text{---Na}^+$ ($113.1 \times n + 23$), with a peak one mass unit of greater of the general form $\text{H}[-\text{NH}-(\text{CH}_2)_5-\text{CO}]_n\text{---Na}^+$ ($113.1 \times n + 1 + 23$). The previously cited works attribute the lower-mass peak to polymer containing cyclic oligomers.^{26–28} In each series, there is a substantial signal for a species 16 Da above the major peak, representing an ion of the form $[-\text{NH}-(\text{CH}_2)_5-\text{CO}]_n\text{---O---Na}^+$ ($113.1 \times n + 16 + 23$). For both samples, the most intense peaks correspond to oligomers with $n = 9\text{--}13$, with no appreciable chemical differences observed between the two dissolved fiber types. The similarity displayed again confirms that the molecular base structure of these two nylons is the same.

Table II. Comparison of Mechanical Properties of Samples

Sample	Elongation (%)	Tenacity (g/den)	Modulus (g/den)
Nylon 6A	12.60 \pm 1.57	2.87 \pm 0.16	29.12 \pm 2.44
Nylon 6B	12.39 \pm 0.71	1.30 \pm 0.07	19.89 \pm 1.26

Mechanical Testing. To investigate further the differences between the extruded C-CP fibers, tensile testing was performed. The response curves of Figure S4 of the Supporting Information reflect the amount of positive strain (tensile) the respective fibers could withstand before breaking. Nylon 6B, on average, withstood a higher load (breaking strength, gf) than nylon 6A. The resulting average elongation, tenacity, and modulus of 10 individual fiber tensile tests are given in Table II. Both fiber samples yielded levels of elongation of $\sim 12\%$. The values for both modulus and tenacity are significantly different as would be expected when considering the difference in deniers of 2.67 and 7.72 for nylon 6A and 6B, respectively. The higher denier sample, in this case nylon 6B, has lower tenacity and modulus, which is a direct result of the spinning process already alluded to. To achieve low denier fibers the wind up speeds are greater and as such more orientation and crystallinity is imparted to the filaments. Hence, much improved mechanical properties are achieved due to the increased alignment and proximity of the polymer chains with one another. These data coupled with that obtained via DSC support this observation.

Determination of Relative Viscometry. The viscosity of dilute polymer solutions is considerably higher than that of the pure solvent. Any observed viscosity increase is dependent on the solvent, the temperature, the molecular chain length, and the polymer concentration. The number average molecular weight (\bar{M}_n) of nylon 6 is related to the number average degree of polymerization, $(\text{DP})_n$, as follows:

$$(\bar{M})_n = 113.16(\text{DP})_n \quad (3)$$

where 113.16 is the molecular weight of caprolactam.

It is possible to use RV as a measure of molecular weight using the following empirical relationship²⁹

$$(\text{DP})_n = 95.70(\text{RV} - 1) \quad (4)$$

RV values of 2.08 and 2.33 were obtained giving corresponding $(\bar{M})_n$ values of 11,695 and 14,403 Da for nylon 6A and 6B, respectively. Clearly a polymer with lower average molecular weight, in this case nylon 6A, will also have a greater number of end groups per unit fiber mass available for chemical interactions. In agreement with the MALDI-MS spectra, nylon 6B has a longer repeating polymer chain and less available end groups to contribute to protein interactions.

Determination of Amino End Group Content. As a final test, the quantification of end groups available on each fiber sample was determined. As described previously, the separation of proteins on nylon 6 C-CP fibers is due to both HICs with the nylon 6 backbone and electrostatic interactions with charged

Table III. Amino End Group Content Determined by a Reaction with Ninhydrin (2,2-Dihydroxyindane-1,3-dione)

Sample	Amino end group content ($\mu\text{mol/g}$)
Nylon 6A	78.6 ± 1.19
Nylon 6B	62.0 ± 1.79

end groups on the fiber surface, having an equal number of amino and carboxy groups. The reaction of primary amines (which *de facto* are end groups) with ninhydrin allows for the quantitative determination of the amino end groups on the fiber. This ninhydrin method, introduced by Knott and Rossbach²¹ in 1980, compares a reaction of ninhydrin and the sample fibers with a reaction of ninhydrin and ϵ -aminocaproic acid, which is an intermediate in the polymerization of nylon 6, resembling the nylon 6 monomer unit. When ninhydrin is in the presence of amino groups, it binds to nitrogen to produce a bluish-purple compound, called Ruhmann purple; the more intense color produced, the greater number of amino end groups are present. This method was chosen over other common methods, such as acid–base titrations, due to the ability to differentiate between primary amine end groups and other basic groups. The number of amino groups can be quantitatively determined from a Beer's Law plot of absorbance values versus concentration of standard, neat ϵ -aminocaproic acid solutions. The sensitivity of this method is due to the reaction medium, which causes the fibers to swell, ensuring that a greater extent of the fiber matrix is reacted.

The results of the ninhydrin reaction determinations (in terms of μmol amino groups per gram of fiber) are presented in Table III. In this case, nylon 6A yields $\sim 25\%$ more amine functionality per unit fiber mass than nylon 6B. Extending this value to the relative amount of fiber mass per column leads to the conclusion that overall the number of amine groups in the nylon 6A column is $\sim 16\%$ greater than the number in the nylon 6B column. As noted, the ninhydrin solvent system is designed to penetrate the porosity of the fiber matrices, while the size of these proteins (with radii of gyration of ~ 4 nm) prohibits their entering the natural fiber porosity. Thus, the relevant charged sites are only those that exist on the fiber surface. Therefore, the 16% higher mass-based end group density, coupled with the $\sim 2\times$ higher fiber surface area per column combine to very effectively yield greater levels of retention based on ionic interactions.

From a correlation of the ninhydrin results with the relative viscometry data, it is strongly suggested that the nylon 6A fibers were extruded from a base polymer having somewhat shorter oligomer lengths, meaning a shorter chain of nylon 6 monomers between end groups. This supports its comparability with the spectral data of dissolved, amorphous samples, and allows for more end groups to be present per unit of fiber mass. Nylon 6B was extruded from a base polymer having longer oligomer length.

CONCLUSIONS

A range of physical and chemical tests has been implemented to compare two nylon 6 C-CP fiber stocks that exhibited different

chromatographic behavior. The nylon 6A C-CP fiber-packed column allowed for a highly efficient separation of a three-protein suite using a steep gradient at a flow rate of 2 mL min^{-1} with all proteins eluting in less than 2 min. Under the same conditions, the nylon 6B C-CP fiber-packed column was unable to fully-retain ribonuclease A, with the cytochrome c and lysozyme components also showing reduced retention. Investigation into the physical structure of the fibers and columns revealed differences in the absolute shape, perimeter/surface area, and denier. Chemical, thermal, and mechanical testing showed differences in crystallinity, strength, molecular weight, and number of amine end groups between the fiber types. In general, while it seems clear that the two fibers are extruded from nylon 6 polymers, based on the FTIR and DSC testing, the thermal and viscometry measurements suggest a process in manufacture of the base nylon 6 polymer, whereby longer oligomer chains are affected. The higher numbered oligomers present in nylon 6B result in fewer end groups per unit fiber mass. A smaller number of surface end groups yields less efficient surface ionic interactions for protein retention, thus the weakly retained ribonuclease A is likely only interacting through hydrophobic means.

Much of the previous work with C-CP fibers was undertaken fully realizing that fiber extrusion conditions would affect the fiber shape, denier, etc., which dictate the column hydrodynamic characteristics. The studies described here point clearly to the importance of base molecular weight and fiber extrusion conditions in affecting the physical and chemical nature of polymer fibers that otherwise originate from identical monomers. It is believed that the knowledge of these effects will allow for a much more thorough understanding of the C-CP fiber platform and optimized paths forward.

ACKNOWLEDGMENTS

This material is based upon work supported by the National Science Foundation Division of Chemistry under Grant No. 1011820 (cofunded by the MPS/CHE, ENG/CBET, and EPSCoR). The technical expertise in the acquisition of the FTIR and DSC data by Ms. Kim Ivey of the Clemson University School of Materials Science and Engineering is gratefully acknowledged.

REFERENCES

1. Putscher, R. E.; Saunders, J. H. In *Kirk-Othmer Encyclopedia of Chemical Technology*; Grayson, M., Ed.; Wiley: Hoboken, NJ, USA, **1982**; p 328.
2. Lewis, D. M. In *Synthetic Fibre Materials*; Brody, H., Ed.; Longman Group: Essex, UK, **1994**.
3. Brody, H. *Synthetic Fibre Materials*; Longman Scientific & Technical: Harlow, Essex, England, **1994**.
4. Fourné, F. *Synthetic Fibers*; Hanser/Gardner: Cincinnati, OH, **1999**.
5. Escandar, G.; Gomez, D.; Mansilla, A.; de la Pena, A.; Goicoechea, H., *Anal. Chim. Acta* **2004**, *506*, 161.
6. Peralta, C.; Fernandez, L.; Masi, A. *Microchem. J.* **2011**, *98*, 39.
7. Pahujani, S.; Kanwar, S.; Chauhan, G.; Gupta, R. *Bioresour. Technol.* **2008**, *99*, 2566.

8. Yang, F.; Weber, T.; Gainer, J.; Carta, G. *Biotechnol. Bioeng.* **1997**, *56*, 671.
9. Aussawasathien, D.; Teerawattananon, C.; Vongachariya, A. *J. Membr. Sci.* **2008**, *315*, 11.
10. Marcus, R. K. *J. Sep. Sci.* **2008**, *31*, 1923.
11. Marcus, R. K. *J. Sep. Sci.* **2009**, *32*, 695.
12. Marcus, R. K.; Davis, W. C.; Knippel, B. C.; LaMotte, L.; Hill, T. A.; Perahia, D.; Jenkins, J. D. *J. Chromatogr. A* **2003**, *986*, 17.
13. Nelson, D. M.; Stanelle, R. D.; Brown, P.; Marcus, R. K. *Am. Lab.* **2005**, *37*, 28.
14. Nelson, D. M.; Marcus, R. K. *Anal. Chem.* **2006**, *78*, 8462.
15. Nelson, D. M.; Marcus, R. K. *Prot. Pept. Lett.* **2006**, *13*, 95.
16. Stanelle, R. D.; Mignanelli, M.; Brown, P.; Marcus, R. K. *Anal. Bioanal. Chem.* **2006**, *384*, 250.
17. Stanelle, R. D.; Straut, C. A.; Marcus, R. K. *J. Chromatogr. Sci.* **2007**, *45*, 415.
18. Stanelle, R. D.; Marcus, R. K. *Anal. Bioanal. Chem.* **2009**, *393*, 273.
19. Stepaniak, R.; Garton, A.; Carlsson, D.; Wiles, D. *J. Polym. Sci. Part B: Polym. Phys.* **1979**, *17*, 987.
20. Neue, U. D. *HPLC Columns: Theory, Technology, and Practice*; Wiley-VCH: New York, **1997**.
21. Knott, J.; Rossbach, V. *Angew. Makromol. Chem.* **1980**, *86*, 203.
22. Rotter, G.; Ishida, H. *J. Polym. Sci. Part B: Polym. Phys.* **1992**, *30*, 489.
23. Huang, L.; Allen, E.; Tonelli, A. *Polymer* **1999**, *40*, 3211.
24. Wunderlich, B. *Macromolecular Physics, Vol. 3: Crystal Melting*; Academic Press: New York, NY, USA, **1980**.
25. Skelton, R.; Dubois, F.; Zenobi, R. *Anal. Chem.* **2000**, *72*, 1707.
26. Montaudo, G.; Montaudo, M.; Puglisi, C.; Samperi, F. *Macromolecules* **1995**, *28*, 4562.
27. Montaudo, G.; Montaudo, M.; Puglisi, C.; Samperi, F. *J. Polym. Sci. A Polym. Chem.* **1996**, *34*, 439.
28. Choi, H.; Choe, E. K.; Yang, E. K.; Jang, W.; Park, C. R. *Bull. Korean Chem. Soc.* **2007**, *28*, 2354.
29. Gupta, V. B.; Kothari, V. K. *Manufactured Fiber Technology*; Chapman and Hall: London, UK, **1997**.